Monte Carlo study of magnetization dynamics in uniaxial ferromagnetic nanowires in the presence of oscillating and biased magnetic fields

Yusuf Yüksel*

Department of Physics, Dokuz Eylül University, Kaynaklar Campus, TR-35160 Izmir, Turkey

(Received 20 October 2014; published 30 March 2015)

We examine the dynamic phase transition properties of ferromagnetic uniaxial nanowires with tunable radius r in the presence of both oscillating and biased magnetic fields. Variation of the transition temperature as a function of amplitude h_0 of the oscillating field has been analyzed in the absence of magnetic bias h_b and at constant oscillation period P. We find that the transition temperature as a function of h_0 exhibits an exponential decay behavior. We also investigate the magnetization dynamics in terms of magnetic hysteresis loops as functions of the parameters h_b, h_0, and P. Our calculations are qualitatively in agreement with the recent experimental results obtained for uniaxial cobalt films in which it was concluded that the bias field h_b is the conjugate field of the dynamic order parameter.

DOI: 10.1103/PhysRevE.91.032149 PACS number(s): 05.70.Ln, 75.40.Mg, 81.07.Gf

I. INTRODUCTION

Dynamic phase transition (DPT) phenomenon in bulk magnetic systems was proposed more than two decades ago [1,2], and since then it has been a focus of interest in statistical mechanics of phase transitions [3,4]. Various bulk and nanostructured systems have been investigated using various methods such as effective field theory (EFT) [5–8] and Monte Carlo (MC) simulations [9–12].

On the experimental side, for a Co(4 Å)/Pt(7 Å) multilayer system with strong perpendicular anisotropy, an example of DPT has been observed by Robb *et al.* [13]. They found that the experimental nonequilibrium phase diagrams strongly resemble the dynamic behavior predicted from theoretical calculations of a kinetic Ising model. Hence, it is clear that there exists a strong evidence of qualitative consistency between theoretical and experimental studies.

Experimentally, rather than applying a sinusoidal magnetic field on the sample, keeping its time sequence stable is a substantial issue. In this regard, several recent studies consider the influence of a time-independent bias field h_b on the DPT characteristics of kinetic ferromagnets. In fact, the pioneering computational work of Robb and coworkers [14] identified the bias field h_b as a significant component of the field conjugate to dynamic order parameter Q and established the existence of a fluctuation-dissipation relation for magnetic susceptibility. Subsequently, their group succeeded in experimentally realizing their theoretical predictions in $[Co/Pt]_3$ magnetic multilayers [13]. Consequently, the importance of magnetic bias field h_b in DPT has been addressed theoretically for two-dimensional kinetic Ising model [15,16], as well as experimentally for uniaxial cobalt films [17].

On the other hand, magnetic nanowires and nanotubes such as ZnO [18], FePt, and Fe_3O_4 [19] can be synthesized by various experimental techniques and they have many applications in nanotechnology [20,21], and they are also utilized as raw materials in fabrication of magnetoresistive devices and perpendicular recording media [22–24]. In this regard, it is worth investigating DPT properties and significance of h_b on DPT characteristics of nanowires for which only equilibrium properties have been recently investigated [25,26].

Microscopic Hamiltonians based on conventional Ising spins are widely used for modeling the magnetic properties of highly anisotropic (uniaxial) materials such as MnF_2. Besides, in order to minimize the magnetostatic energy, the easy axis magnetization direction of magnetic nanowires is generally along the wire axis [27,28]. In other words, in the case of highly anisotropic (i.e., uniaxial) materials, magnetic dipole moments align along a particular direction (i.e., z direction). This fact allows us to simulate uniaxial ferromagnetic nanowires using Ising spins. As will be discussed in the following sections, the results obtained in the present paper show that the experimental findings obtained in Ref. [17] for ferromagnetic thin films (especially, variation of Q as a function of h_b) can also be qualitatively verified for ferromagnetic nanowires within a simple Ising model.

The paper is organized as follows: In Sec. II, we briefly introduce our model and simulation procedure. Section III is devoted to discussion of simulation results, and in Sec. IV we outline our conclusions.

II. MODEL AND SIMULATION DETAILS

For the present problem, we consider a cylindrical nanowire placed along the z axis with length L and radius r as depicted in Fig. 1 and we focus our attention on the uniaxial ferromagnetic nanowires, which can be represented by the following microscopic Hamiltonian:

$$\mathcal{H} = -J \sum_{\langle ij \rangle} S_i S_j - h(t) \sum_i S_i, \tag{1}$$

where $S_i = \pm 1$ is the z component of the Pauli spin operator and J denotes the exchange interaction between neigboring spins. The last term in Eq. (1) is taken over all lattice sites and it represents the interactions due to the time-dependent external field $h(t)$, which has the form

$$h(t) = h_b + h_0 \cos \omega t, \tag{2}$$

*yusuf.yuksel@deu.edu.tr

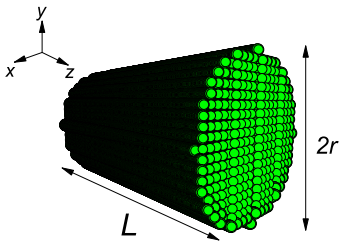

FIG. 1. (Color online) Schematic representation of a cylindrical nanowire with length L and radius r.

where h_b is the bias of the external field and h_0 denotes the oscillation amplitude. Oscillation period P is defined as $P = 2\pi/\omega$, where ω is the angular frequency of the oscillating field.

In the simulation procedure, we apply metropolis Monte Carlo (MC) sampling technique [29] with sequential sweeping procedure and define periodic (free) boundary conditions in the planes parallel (perpendicular) to the wire axis. Several runs with $L = 400$ did not produce significant difference on the location of the transition temperature, hence the wire length with $L = 200$ layers was found to be sufficient to reduce the finite-size effects along the wire axis. The time dependence of magnetic field, i.e., period P of the oscillating external field is defined in terms of Monte Carlo steps (MCSs) in such a way that $P = \kappa$, where κ is the number of MCSs necessary for one complete cycle of the oscillating field. This choice allows us to define the time-dependent magnetic fields in discretized steps. In the simulation process, the first 100 cycles were discarded for thermalization, and data were collected over the next 100 cycles of the external field. In addition, in order to reduce the statistical errors, 50–200 independent measurements were performed for any given set of system parameters.

Following Refs. [2] and [4], instantaneous magnetization is defined as

$$M(t) = \frac{1}{N}\sum_{i=1}^{N} S_i, \tag{3}$$

where N is the number of spins, which depends on the wire radius in our model. Using Eq. (3), dynamic order parameter Q can be written as

$$Q = \frac{1}{P}\oint M(t)dt. \tag{4}$$

In order to estimate the transition temperature of the system, we also calculate the variance in $|Q|$, namely [11,30,31],

$$\Delta\mathcal{M} = N\mathrm{Var}(|Q|) = N[\langle Q^2\rangle - \langle|Q|\rangle^2], \tag{5}$$

from which magnetic susceptibility follows as $\chi = \Delta\mathcal{M}/T$.

III. RESULTS AND DISCUSSION

A. Edge effects due to finite cross-section in equilibrium

First of all, let us investigate the boundary effects due to the finite cross-section of the wire (see Fig. 2). In Fig. 3, we plot the hysteresis loops of equilibrium system with some selected values of wire radius r at a temperature $T/J = 1.0$. In the limit $r \to 0$, the model reduces to one-dimensional Ising model with $L = 200$ spins, which does not have an ordered ground state at $T > 0$. In this regard, our results fit well with the exact

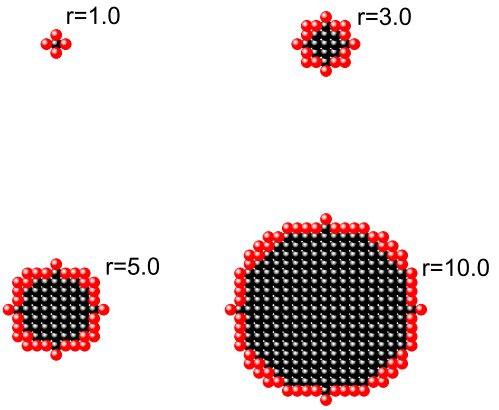

FIG. 2. (Color online) Top view of several nanowire systems simulated with different cross-sections. Black (red) dots represent interior (surface) spins.

solution [32] (cf. solid line in Fig. 3) when $r = 0.0$. Along with increasing the wire thickness at a finite temperature, hysteresis loops with nonzero coercivity originate, which is a peculiar behavior of ferromagnetic materials. This can be attributed to the lattice parameter, i.e., the coordination number q of the system. Namely, for $r = 0.0$, the system is a linear chain with $q = 2$. On the other hand, for thicker wires (even for $r = 1.0$), interior spins have six nearest neighbors, hence it allows the system to establish an ordered phase for $r \geqslant 1.0$, which shows itself as wider hysteresis loops with increasing cross-section.

In Fig. 4, we examine the thermal variation of the order parameter $|Q|$ and susceptibility χ in equilibrium (in this case $|Q|$ is the absolute value of the time averaged magnetization, instead of dynamic order parameter since $h_0/J = h_b/J = 0.0$) as a function of wire radius r. Edge effects can be clearly observed. Namely, the curves depicted in Fig. 4(a) become smeared out as the wire radius decreases. Corresponding magnetic susceptibility curves are also plotted in Fig. 4(b).

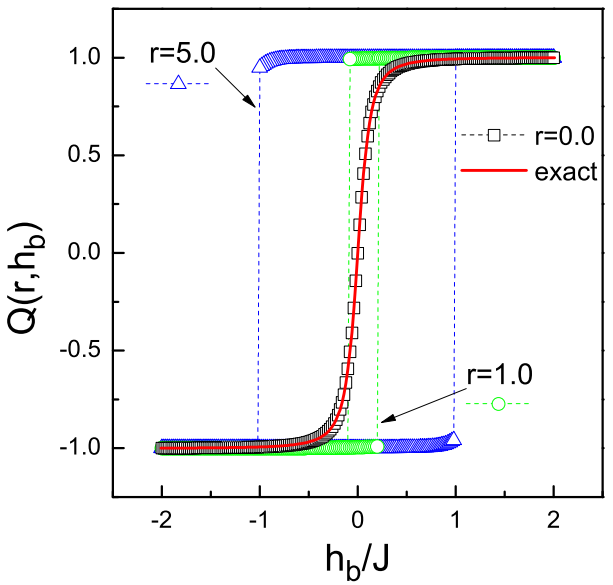

FIG. 3. (Color online) Hysteresis loops of equilibrium system ($h_0/J = 0.0$) at $T/J = 1.0$ with some selected values of wire radius r.

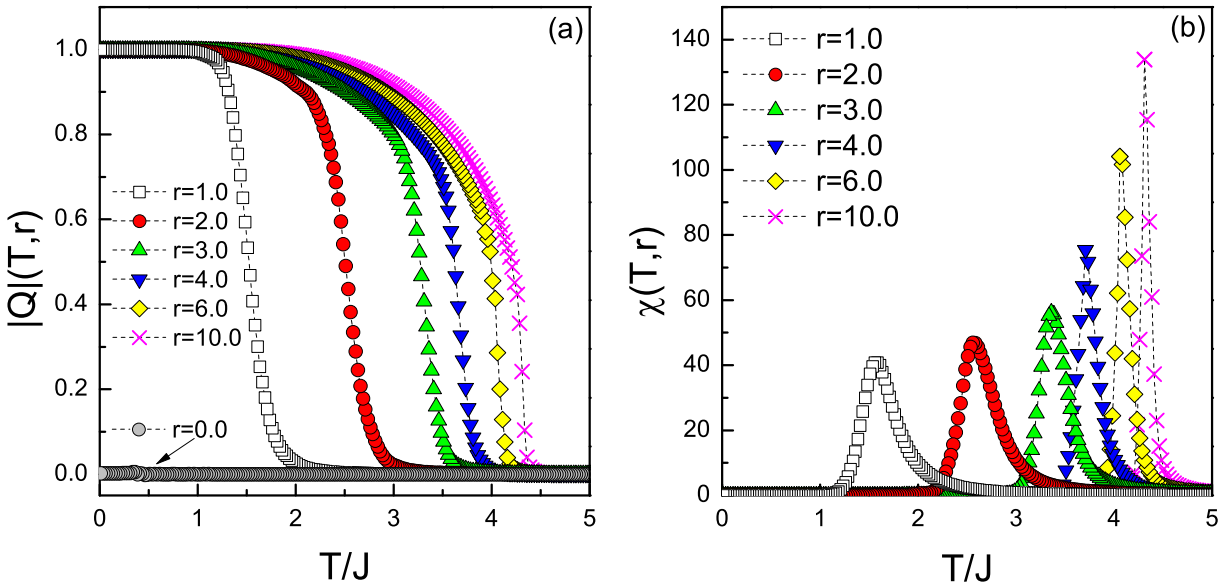

FIG. 4. (Color online) Temperature dependence of (a) absolute value of the order parameter $|Q|$, (b) magnetic susceptibility χ as a function of wire radius with $h_0/J = 0.0$ and $h_b/J = 0.0$.

As seen from this figure, susceptibility curves exhibit a smooth cusp for thinner wires. As the cross-section of the wire increases then a divergent behavior originates in these susceptibility curves at the transition temperature, indicating a second-order phase transition. Therefore, in the following discussions regarding the nonequilibrium phase transitions of the system, in order to reduce these edge-effects due to small radius, we will work on ferromagnetic nanowires with $r = 10.0$ containing $N = 63\,400$ lattice sites.

B. Dynamic phase transition properties

Dynamic phase diagram of ferromagnetic nanowires with $r = 10.0$ in a $(T_c/J - h_0/J)$ plane in the absence of bias fields is shown in Fig. 5. Transition temperature values were determined by examining the maxima of susceptibility curves. According to Fig. 5, transition temperature exhibits a decreasing behavior with increasing h_0 values as a consequence of the following physical mechanism: For small amplitude values, the energy supplied by the periodic magnetic field cannot compensate the ferromagnetic energy due to the nearest-neighbor coupling J at low temperatures. Hence, a dynamic phase transition cannot be observed unless a relatively large amount of thermal energy is supplied to the system. As the field amplitude increases, it becomes dominant against the ferromagnetic nearest-neighbor bonds, and a dynamic phase transition can be observed at low temperatures. We note that T_c/J does not linearly decrease with increasing h_0/J but exhibits an exponential decay behavior that can be well characterized by the following analytical expression:

$$T_c \propto \exp(-h_0/\alpha). \tag{6}$$

An exponential fit of our numerical data (see the dashed line in Fig. 5) according to Eq. (6) yields $\alpha = 1.292 \pm 0.051$.

The temperature dependencies of dynamic order parameter Q and magnetic susceptibility χ curves as functions of h_0/J corresponding to the dynamic phase diagram in Fig. 5 are plotted in Fig. 6. One can clearly see from this figure that the order parameter Q decreases with increasing temperature and vanishes at $T = T_c$ and the susceptibility curves exhibit enhanced maxima, which are observed at lower temperature values with increasing h_0 values.

Finally, in Fig. 7, we present 2D-contour plots of the difference $\Delta Q = Q^d - Q^i$ in $(h_0/J - h_b/J)$ and $(P - h_b/J)$ planes where Q^d and Q^i are the decreasing and increasing field branches of hysteresis loops. The triangular regions depicted in Figs. 7(a) and 7(b) correspond to ferromagnetic phases with nonzero coercivity. Value of coercive field decreases

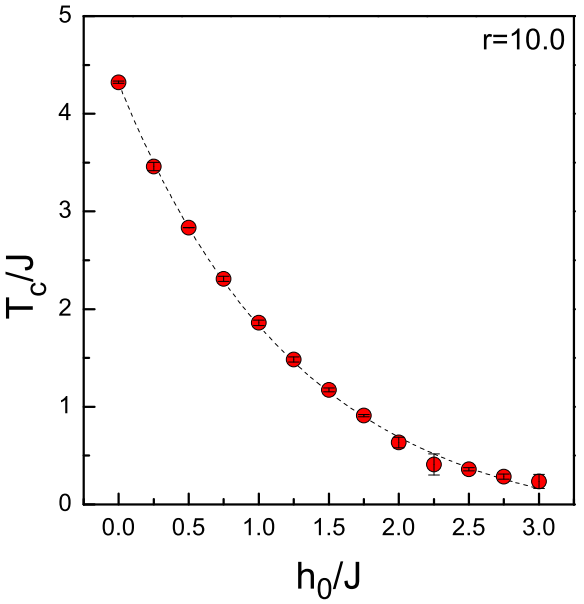

FIG. 5. (Color online) Dynamic phase diagram in $(h_0/J - T_c/J)$ plane for a nanowire with radius $r = 10.0$. Oscillation period of the external field is selected as $P = 100$.

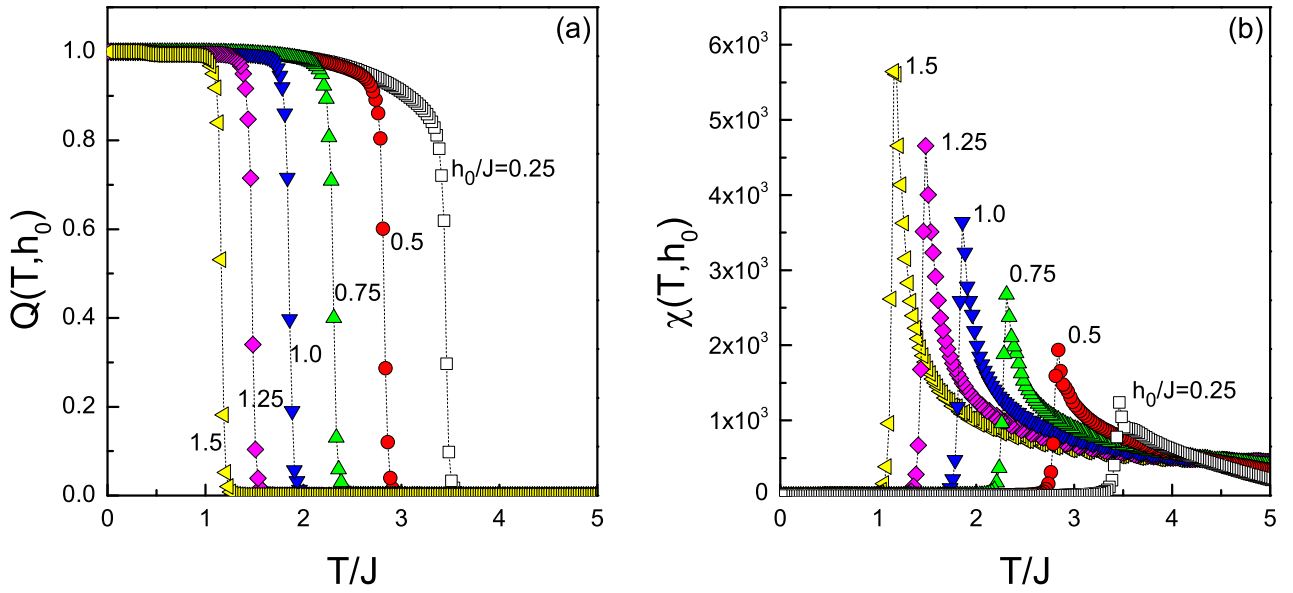

FIG. 6. (Color online) Temperature dependence of (a) dynamic order parameter Q, (b) magnetic susceptibility χ as a function of h_0/J with $r = 10.0$, $P = 100$, and $h_b/J = 0.0$.

linearly and vanishes at a critical field and critical period, respectively, at which the nanowire exhibits paramagnetic behavior. A similar investigation was carried out in Ref. [17], and the authors revealed similar results in $(h_b/J - P)$ plane experimentally for uniaxial cobalt films of 30 nm thick. They also verified their results theoretically using mean-field theory. We conclude from Fig. 7 that in accordance with the results presented in Ref. [17], we can claim that bias field h_b is the conjugate field of the dynamic order parameter Q.

IV. CONCLUSIONS

In conclusion, using MC simulation technique, we studied the nonequilibrium phase transition properties of a uniaxial ferromagnetic nanowire system in the presence of both oscillating and biased magnetic fields. After analyzing the boundary effects in equilibrium, we have obtained the phase diagram of a nanowire with radius $r = 10.0$ in a $(T_c/J - h_0/J)$ plane in the presence of oscillating magnetic fields. According to our results, transition temperature of the system does not show a linear decreasing behavior but exhibits an exponential decay with increasing amplitude h_0/J. In addition, we have also clarified the thermal variation of dynamic order parameter Q, as well as magnetic susceptibility χ as functions of h_0/J.

Finally, we have discussed the influences of the oscillation amplitude h_0/J and period P of the external field on the hysteresis loops of the system. Our results yield that bias field h_b is the conjugate field of the dynamic order parameter Q, which is also in a good agreement with the recent

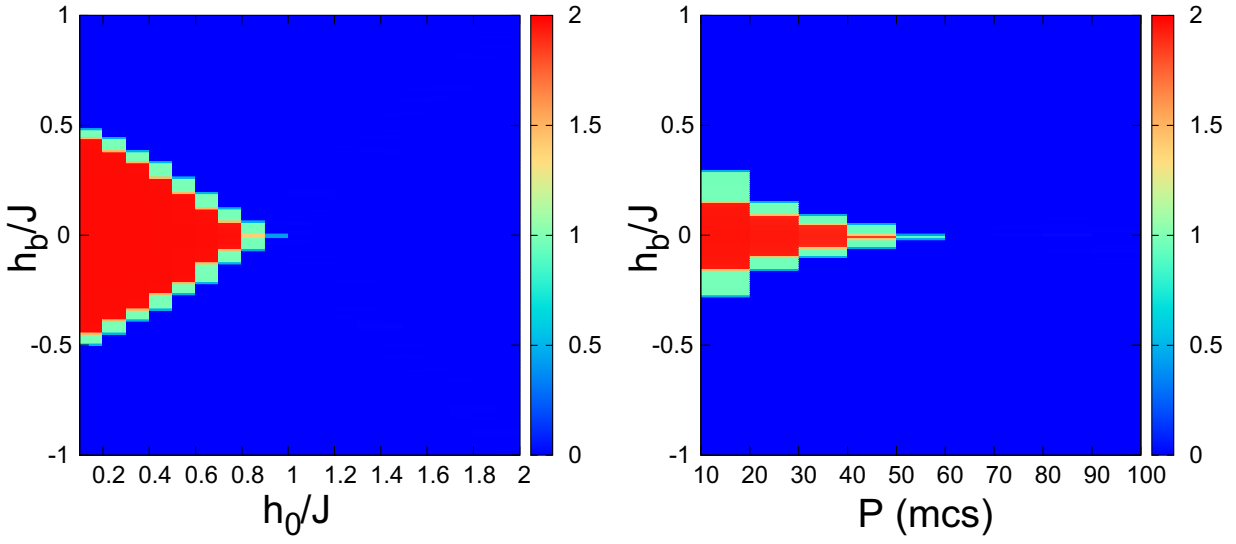

FIG. 7. (Color online) Variation of ΔQ in 2D contour representation in (a) $(h_0/J - h_b/J)$ plane with $P = 100$ and (b) $(P - h_b/J)$ plane with $h_0/J = 1.0$, respectively. The other system parameters are fixed as $r = 10.0$ and $T/J = 2.0$.

theoretical mean field analysis and also with the experimental results regarding the ferromagnetic uniaxial cobalt films, indicating that dynamic phase transitions and equilibrium critical phenomena have a great many similar features. In addition, most of the results reported in the present work are shown to be not model-specific type but generic phenomena observed in dynamic magnetic systems.

ACKNOWLEDGMENTS

The author thanks Andreas Berger from CIC Nanogune for critical reading of the paper and for valuable discussions on the subject. The numerical calculations reported in this paper were performed at TUBITAK ULAKBIM High Performance and Grid Computing Center (TR-Grid e-Infrastructure).

[1] T. Tomé and M. J. de Oliveira, Phys. Rev. A **41**, 4251 (1990).
[2] W. S. Lo and R. A. Pelcovits, Phys. Rev. A **42**, 7471 (1990).
[3] M. Acharyya, Int. J. Mod. Phys. C **16**, 1631 (2005), and references therein.
[4] B. K. Chakrabarti and M. Acharyya, Rev. Mod. Phys. **71**, 847 (1999), and references therein.
[5] B. Deviren, O. Canko, and M. Keskin, Chin. Phys. B **19**, 050518 (2010).
[6] Y. Yüksel, E. Vatansever, Ü. Akıncı, and H. Polat, Phys. Rev. E **85**, 051123 (2012).
[7] B. O. Aktas, Ü. Akıncı, and H. Polat, Thin Solid Films **562**, 680 (2014).
[8] E. Kantar and M. Ertas, Superlattice Microst. **75**, 831 (2014).
[9] G. M. Buendía and P. A. Rikvold, Phys. Rev. E **78**, 051108 (2008).
[10] Y. Yüksel, E. Vatansever, and H. Polat, J. Phys.: Condens. Matter **24**, 436004 (2012).
[11] H. Park and M. Pleimling, Phys. Rev. E **87**, 032145 (2013).
[12] M. Boughrara, M. Kerouad, and A. Zaim, J. Magn. Magn. Mater. **368**, 169 (2014).
[13] D. T. Robb, Y. H. Xu, O. Hellwig, J. McCord, A. Berger, M. A. Novotny, and P. A. Rikvold, Phys. Rev. B **78**, 134422 (2008).
[14] D. T. Robb, P. A. Rikvold, A. Berger, and M. A. Novotny, Phys. Rev. E **76**, 021124 (2007).
[15] O. Idigoras, P. Vavassori, and A. Berger, Physica B **407**, 1377 (2012).
[16] R. A. Gallardo, O. Idigoras, P. Landeros, and A. Berger, Phys. Rev. E **86**, 051101 (2012).
[17] A. Berger, O. Idigoras, and P. Vavassori, Phys. Rev. Lett. **111**, 190602 (2013).
[18] Z. Fan and J. G. Lu, Int. J. High Speed Electron. Syst. **16**, 883 (2006).
[19] Y. C. Su, R. Skomski, K. D. Sorge, and D. J. Sellmyer, Appl. Phys. Lett. **84**, 1525 (2004).
[20] R. Skomski, J. Phys.: Condens. Matter. **15**, R841 (2003).
[21] H. Schlörb, V. Haehnel, M. S. Khatri, A. Srivastav, A. Kumar, L. Schultz, and S. Fähler, Phys. Status Solidi B **247**, 2364 (2010).
[22] J.E. Wegrowe, D. Kelly, Y. Jaccard, Ph. Guittienne, and J.-Ph. Ansermet, Europhys. Lett. **45**, 626 (1999).
[23] A. Fert and L. Piraux, J. Magn. Magn. Mater. **200**, 338 (1999).
[24] S. D. Bader, Rev. Modern Phys. **78**, 1 (2006).
[25] T. Kaneyoshi, Phys. Status Solidi B **248**, 250 (2011).
[26] A. Feraoun, A. Zaim, and M. Kerouad, Physica B **445**, 74 (2014).
[27] M. Mathews, R. Jansen, G. Rijnders, J. C. Lodder, and D. H. A. Blank, Phys. Rev. B **80**, 064408 (2009).
[28] R. P. Cowburn, J. Phys. D: Appl. Phys. **33**, R1 (2000).
[29] N. Metropolis, A. W. Rosenbluth, M. N. Rosenbluth, A. H. Teller, and E. Teller, J. Chem. Phys. **21**, 1087 (1953).
[30] S. W. Sides, P. A. Rikvold, and M. A. Novotny, Phys. Rev. Lett. **81**, 834 (1998).
[31] H. Park and M. Pleimling, Phys. Rev. Lett. **109**, 175703 (2012).
[32] R. K. Pathria, *Statistical Mechanics*, 2nd. ed. (Butterworth-Heinemann, Oxford, 1996), p. 366.